JOURNAL OF SOLID STATE CHEMISTRY 10, 183–194 (1974)

Oxidative Nonstoichiometry in Perovskites, an Experimental Survey; the Defect Structure of an Oxidized Lanthanum Manganite by Powder Neutron Diffraction

B. C. TOFIELD* AND W. R. SCOTT

The Inorganic Chemistry Laboratory, University of Oxford, South Parks Road, Oxford OX1 3QR, England

Received August 21, 1973

Oxide perovskites showing oxidative nonstoichiometry (ABO_{3+x}) have been investigated. The structure of $LaMn^{3+}_{0.76}Mn^{4+}_{0.24}O_{3.12}$ has been investigated by powder neutron diffraction and a composition $(La_{0.94\pm0.02}\square_{0.06\pm0.02})(Mn^{3+}_{0.745}Mn^{4+}_{0.235}\square_{0.02})O_3$ with partial elimination of La_2O_3 and vacancies on both the A and B metal sites determined. A much smaller degree of nonstoichiometry has been found for $LaVO_{3+x}(x \leqslant 0.05)$, and $LaCrO_3$, $LaFeO_3$, and $EuTiO_3$ did not show nonstoichiometry under the conditions used. A single phase region from $Ba_{0.8}La_{0.2}Ti^{4+}_{0.8}Ti^{3+}_{0.2}O_{3.0}$ to $Ba_{0.8}La_{0.2}Ti^{4+}O_{3.1}$ has been confirmed for lanthanum-doped $BaTiO_3$, but the solubility of La^{3+} in $SrTiO_3$ is very small; consideration of the ionic radii indicates that the dopant ion of higher oxidation state must be significantly smaller than the normal ion to stabilize a wide nonstoichiometric region with B site vacancies. The extensive nonstoichiometry shown by $LaMnO_{3+x}$, in contrast to the other lanthanum-transition–metal perovskites $LaBO_3$, may result from the much larger reduction in ionic radius from Mn^{3+} to Mn^{4+} than is found for other transition-metal ions.

Introduction

In addition to the extensive family of stoichiometric perovskites of general formula ABX_3, many such compounds exhibit nonstoichiometry on one or more sublattices (*1*). Systems with A cation deficiency have been widely investigated, and the existence of anion deficiency is well established in several oxide systems. B cation nonstoichiometry, however, does not appear to be known,[1] except for lanthanum-doped lead titanate recently studied by Hennings and Rosenstein (*2*). This may not seem surprising on the electrostatic model as the B cations are smaller and often have a higher formal charge than the A cations.

There are, however, other oxide systems with reported composition ABO_{3+x} that cannot be rationalized on the basis of solely A cation and/or oxide vacancies. These include $La(Mn^{3+}_{1-2x}Mn^{4+}_{2x})O_{3+x}$ (*3*), $(Ba^{2+}_{1-2x}La^{3+}_{2x})Ti^{4+}O_{3+x}$ (*4*), and $(Eu^{2+}_{1-2x}Eu^{3+}_{2x})Ti^{4+}O_{3+x}$ (*5*). Without anticipating the defect structures which may be determined, we term this behavior oxidative nonstoichiometry. None of these compounds has been studied by techniques more sensitive than powder X-ray diffraction.

Assuming the existence of such nonstoichiometric perovskites, at least three limiting schemes of behavior are possible: (a) Interstitial oxygen may be present, occupying, probably, $(\frac{1}{2}00)$ sites of low electrostatic potential (of the primitive perovskite cube) (Fig. 1) or perhaps the smaller tetrahedral sites in the AO_3 lattice $(\frac{1}{4}\frac{1}{4}\frac{1}{4})$ (Fig. 1). Such behavior is not common in oxides, although known in nonstoichiometric fluorites such as

* Turner and Newall Research Fellow. Present address: Bell Telephone Laboratories, Holmdel, New Jersey 07733.

[1] Although we might remember that the K_2PtCl_6 structure is stable with 50% B site vacancies.

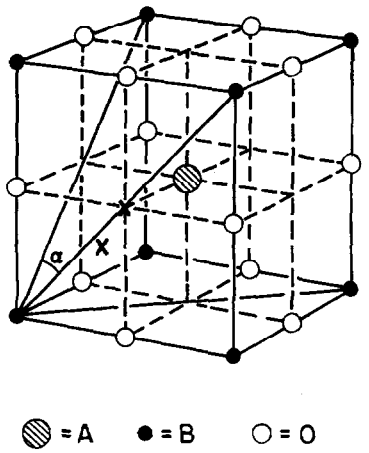

FIG. 1. The perovskite structure ABO_3. The possible interstitial sites (X) are at $(\frac{1}{2}00)$ and $(\frac{1}{4}\frac{1}{4}\frac{1}{4})$. The axes of the primitive rhombohedral cell are indicated. For no rhombohedral distortion $\alpha = 60°$.

UO_{2+x} (*6*). (b) Alternatively, vacancies may exist on both A and B cation sites to leave a perfect oxide sublattice, or (c) the apparent oxygen nonstoichiometry may be completely compensated by A site vacancies only. In this case migration of A cations to complete the B cation sublattice is necessary. Some double perovskites, e.g., Sr_2SrWO_6 (*7*), are known to have the same cations on both B as well as A sites.[2] The stoichiometries in the three cases are ABO_{3+x}, $A_{3/(3+x)}B_{3/(3+x)}O_3$ and $A_{(3-x)/(3+x)}(B_{3/(3+x)}A_{x/(3+x)})O_3$, respectively.

Of course, the formation of a second phase is another means of maintaining perfect B cation and oxygen sublattices at the expense of vacancies on the A cation sublattice only. For example, in the case of $LaMnO_{3+x}$ we may write:

$$La(Mn^{3+}_{1-2x}Mn^{4+}_{2x})O_{3+x} \rightarrow \tfrac{1}{3}xLa_2O_3 + La_{1-2x/3}(Mn^{3+}_{1-2x}Mn^{4+}_{2x})O_3. \quad (1)$$

In such a situation, however, we would expect to detect the second phase either by diffraction methods or optically.

In this work we report the investigation of the structure of $LaMnO_{3.12}$ by powder neutron diffraction and the study of some other systems.

[2] We are aware of no case where the smaller B cations occupy A sites. This unlikely situation is not indicated by the neutron diffraction refinement.

$LaMnO_{3.0}$ is orthorhombic ($a = 5.537$ Å, $b = 5.743$ Å, $c = 7.695$ Å, $c/\sqrt{2} = 5.441$ Å) (*8*). The order of lattice parameters $c/\sqrt{2} < a < b$, characteristic of O′-perovskites (*1*) is a consequence of the Jahn–Teller distortion of the oxide octahedron around the d^4 Mn^{3+} cation. The atomic positions have been determined in space group *Pbnm* by powder neutron diffraction and confirm this distortion (*8*): the three Mn—O distances are 1.905 Å, 1.959 Å, and 2.187 Å; average 2.017 Å.

In the absence of specific Jahn–Teller effects large distortions in the BO_6 octahedra are not generally observed in perovskites, although off-center displacements of B cations occur for some d^0 ions often giving polar phases [e.g., for ferroelectric $BaTiO_3$ at room temperature an ⟨001⟩ Ti displacement results in a tetragonal unit cell (*9*)]. In the usual case that the A cations are smaller than necessary to stabilize the ideal cubic structure, the BO_6 octahedra rotate to produce a lowering of symmetry and a distortion of the oxide coordination around the A cation.

One type of distortion involves rotations about both the ⟨110⟩ and ⟨001⟩ cubic directions (*10*) giving the orthorhombic O–perovskite structure (*1*) (space group *Pbnm*) with lattice parameters $a < c\sqrt{2} < b$, in contrast to $LaMnO_3$.[3] Smaller deviations from cubic symmetry are usually brought about by rotation of the octahedra about a trigonal ⟨111⟩ axis of the perovskite cube (Fig. 2) giving rhombohedral symmetry (space group $R\bar{3}c$, or $R3c$ in the case of off-center distortions by cations). This appears to be the situation in $LaMnO_{3+x}$ for $x > 0.105$, where the oxidation of some Mn^{3+} to Mn^{4+} ions reduces the energy tending to produce long-range Jahn–Teller ordering.

A region of oxidative nonstoichiometry $0 < x < 0.15$ for $LaMnO_{3+x}$ was reported by Wold and Arnott (*3*) with a change in symmetry (at room temperature) from ortho-

[3] It has been pointed out, however, that $a = c/\sqrt{2}$ for zero rotation about ⟨001⟩ and that the small distortions in the BO_6 octahedra that inevitably occur can allow $c/\sqrt{2} < a < b$ for small orthorhombic distortions even in the absence of Jahn-Teller effects; this is observed in $BaCeO_3$ and $BaPrO_3$ (*10*).

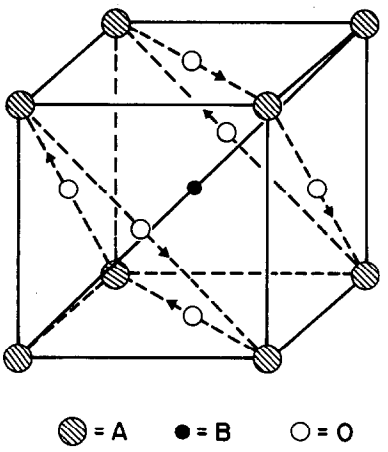

FIG. 2. The displacements of the oxygen atoms for a rhombohedral distortion of the perovskite structure. The BO_6 octahedron rotates about the ⟨111⟩ axis.

rhombic to rhombohedral for an Mn^{4+} concentration greater than 21 %($LaMnO_{3.105}$). The maximum Mn^{4+} content (30%) was obtained by heating the samples at 1100°C in oxygen for 6 days, and the transition temperature from the orthorhombic to rhombohedral phase was found to change from 600°C for $LaMnO_{3.00}$ to about −90°C for $LaMnO_{3.15}$. From the cell parameters quoted we find the volume per formula unit $LaMnO_{3+x}$ (V_f) to decrease with increasing oxidation from 61.17 Å^3 for $x = 0$ to 60.24 Å^3 ($x = 0.048$), 59.30 Å^3 ($x = 0.099$), and 58.79 Å^3 ($x = 0.15$).

Elemans et al. (*8*) showed that a decrease in both the distortion of the unit cell and of the Mn—O octahedron also occurs when the oxidation of Mn^{3+} to Mn^{4+} is compensated by an equivalent substitution of a divalent A cation for La^{3+}. The average Mn—O bond length also decreases as expected. For example, for $La_{0.95}Ba_{0.05}Mn^{3+}_{0.95}Mn^{4+}_{0.05}O_{3.0}$, $a = 5.548$ Å, $b = 5.638$ Å, $c = 7.737$ Å, $V_f = 60.50$ Å^3, average Mn—O distance = 2.000 Å.

$LaMnO_{3+x}$

$LaMnO_{3.12}$ Sample Preparation

Starting materials were La_2O_3 and Mn_3O_4. (All chemicals were Specpure supplied by Johnson-Matthey Chemicals Ltd.) The La_2O_3 was dried at 1000°C *in vacuo* and transferred to a nitrogen-filled dry-box. The Mn_3O_4 was converted to Mn_2O_3 by firing in an oxygen atmosphere at 800°C for 24 hours (the weight gain confirming the composition as $Mn_2O_{2.996\pm0.005}$). The materials were mixed in a 1:1 molar ratio in the dry-box (to prevent pick-up of moisture during mixing; the weight change during firing could then be used as a check on stoichiometry). A sample of composition $LaMnO_{3.12\pm0.01}$ was prepared by firing in oxygen twice at 1200°C and finally at 1100°C (with regrinding in the dry-box between firings). No annealing was attempted after the final firing. The composition was confirmed by analysis of the oxidizing power of the sample by oxidation of I^- ($Mn^{4+}/Mn^{3+} \rightarrow Mn^{2+}$) and determination of the liberated iodine with thiosulfate. (The gravimetric and chemical analyses almost always agreed to the second decimal place in the oxygen contents for the various samples.)

All observed reflections, both on a Debye–Scherrer X-ray photograph (11.46-cm diameter camera, Cu$K\alpha$ radiation used throughout this work) and in the neutron powder pattern (below) were indexed on the basis of a primitive rhombohedral cell (Fig. 1; $a = 5.471 \pm 0.001$ Å, $\alpha = 60°40' \pm 1'$). The alternative face-centered rhombohedral cell, which is more clearly related to a doubled perovskite cube, has dimensions $a = 7.776$ Å, $\alpha = 90°31'$, in good agreement with $a = 7.784$ Å and $\alpha = 90°36'$ given by Wold and Arnott (*3*) for the same stoichiometry.

Phases deficient in lanthanum may be prepared as has been observed for the lanthanum titanates and vanadates (*11*, *12*). For example, with an La:Mn ratio of 0.93:1 (corresponding closely to one product of the reaction:

$$LaMnO_{3.12} \rightarrow La_{0.92}MnO_3 + 0.04La_2O_3 \quad (2))$$

the X-ray pattern is very similar to that observed for $LaMnO_{3.12}$. Elimination of PbO was also observed in certain situations for La^{3+}-doped $PbTiO_3$ (*2*, *13*), and it is thus important to look carefully for La_2O_3 during the preparation of oxidized lanthanum manganites. Because of the sensitivity of the rare-earth oxides to moisture, it could well be

overlooked given the normal atmospheric exposure of a sample before and during X-ray studies. Part of the product, therefore, was reheated to both 1300°C and 1100°C for 24 hours, and after rapid cooling with the furnace (1–2 hours) to about 600°C, removed and loaded into Lindemann tubes for X-ray studies (La_2O_3 is not significantly affected by such a procedure). No changes or new lines were observed in either photograph, indicating that elimination of La_2O_3 was unlikely to have occurred, at least to the extent described by Eq. (2). By comparison, in the case of $La_{0.2}Sr_{0.8}TiO_{3.1}$ (see below) where the La_2O_3 was not significantly soluble, La_2O_3 lines were clearly visible even in the normal mode of X-ray exposure using a glass fiber. Also, in contrast to more highly oxidized samples, no changes were noticed in the powder pattern of $LaMnO_{3.12}$ either after 2 months storage at room temperature or after annealing in a sealed silica tube for 5 days at 500°C.

Such X-ray studies are not definitive, however. The more powerful neutron diffraction study is more illuminating with regard to the structural composition of $LaMnO_{3.12}$.

Other Compositions

It was observed that the simple rhombohedral structure is obtained only if $LaMnO_{3+x}$ is cooled fairly rapidly after firing in oxygen. Extra lines appear both in X-ray photographs and neutron powder patterns for samples annealed in oxygen below 800°C.

The stoichiometry and cell dimensions were not observed to vary very widely with the firing temperature under 1 atm of oxygen. Two firings at 1200°C gave a composition $LaMnO_{3.11\pm0.01}$ ($a = 5.475 \pm 0.001$ Å, $\alpha = 60°38' \pm 1'$) and annealing of this sample for 2 days at 800°C gave $LaMnO_{3.13\pm0.01}$ ($a = 5.471 \pm 0.001$ Å, $\alpha = 60°38' \pm 1'$). Firing at 600°C and 130 atm pressure of oxygen for 1 week, however, increased the Mn^{4+} content to 40% ($LaMnO_{3.20\pm0.01}$) with a significant decrease in unit cell volume ($a = 5.451 \pm 0.001$ Å, $\alpha = 60°30' \pm 1'$, $V_f = 57.91$ Å^3). This represents an extension of the nonstoichiometry previously observed.

The powder X-ray patterns for both $LaMnO_{3.13}$ and $LaMnO_{3.20}$ were similar to that of $LaMnO_{3.12}$ and indexed accordingly as described (it should be noted that the observed splittings of the "cubic" perovskite lines are not consistent with an orthorhombic distortion). Both samples, however, showed faint extra lines below $2\theta = 90°$ which, although indexable on a doubled cubic perovskite cell, are not allowed in the rhombohedral space groups $R\bar{3}c$ or $R3c$. After a period of weeks at room temperature (in stoppered sample bottles) three or four more lines, again related to the principal reflections, were observed at low angle. This did not appear to be accompanied by any significant changes in lattice parameter or stoichiometry.

Neutron Diffraction

The neutron diffraction measurements were made at room temperature on a diffractometer in the reactor PLUTO at A.E.R.E., Harwell. The wavelength was 1.522 Å obtained using a take-off angle of 72° from the (331) plane of a germanium monochromator. The sample was contained in a thin-walled vanadium can.

Nineteen intensities (to $2\theta = 105°$) were determined and refined to obtain scale factor, isotropic temperature factors and oxygen positions. Absorption and extinction effects were small, and no corrections were necessary. The scattering lengths used were $b_{La} = 0.83 \times 10^{-14}$ *m* and $b_O = 0.577 \times 10^{-14}$ *m*, (*14*) and $b_{Mn} = -0.374 \times 10^{-14}$ *m* (*15*).

Several models reflecting the defect situations discussed in the Introduction were tested. The results strongly indicate that the structural situation in $LaMnO_{3.12}$ involves a partial elimination of La_2O_3 leaving vacancies principally on the lanthanum sites but to a certain extent also on the manganese sites, according to Eq. (3):

$$LaMnO_{3.12} \rightarrow 0.02La_2O_3 + La_{0.96}MnO_{3.06},$$
$$La_{0.96}MnO_{3.06} \equiv La_{0.94}Mn_{0.98}O_{3.00}. \quad (3)$$

Refinements were made in space group $R\bar{3}c$ (except where testing the acentric space group $R3c$) with two molecules in the primitive rhombohedral cell, and all converged after four cycles. All nineteen intensities were used

TABLE I

CATION VACANCY REFINEMENTS FOR $LaMnO_{3.12}$

Model	Oxygen position	Determined stoichiometry	Agreement factor (%)
1. $La_{0.96}Mn_{0.96}O_3$	-0.3024 ± 0.0004		1.57
2. $La_{0.92}[Mn_{0.96}La_{0.04}]O_3$	-0.3023 ± 0.0005		1.65
3. $La_{0.92}MnO_3$	-0.3023 ± 0.0005		1.65
4. Allow A site (La) and B site (Mn) occupation numbers to vary from 2	-0.3023 ± 0.0005	$La_{0.95\pm0.02}Mn(La)_{0.96\pm0.04}O_3$	1.48
5. Allow La occupation number to vary from 3	-0.3024 ± 0.0005	$La_{0.94\pm0.02}MnO_3$	1.60
6. $La_{0.96}Mn_{0.98}O_3$	-0.3024 ± 0.0005		1.65
7. Allow La occupation number to vary from 6	-0.3024 ± 0.0005	$La_{0.94\pm0.02}Mn_{0.98}O_3$	1.45

and the function minimized was $\sum w_i(I_{obs} - I_{calc})^2$, where $w = 1/\sigma^2$. The agreement factors are based on intensities.

It was immediately clear that the nonstoichiometry involved cation vacancies rather than oxygen interstitials. All cation vacancy models gave agreement factors lower than 2%, a refinement assuming the stoichiometric formula $LaMnO_{3.0}$ gave poorer agreement ($R = 2.4\%$), and models based on the situations with interstitial oxygen gave agreement factors over 4%. Moreover, on allowing the oxygen occupation numbers to vary, the interstitial atoms were completely removed and the normal oxygen occupation number increased to values agreeing with the cation vacancy models, the R factors dropping to 1.6 and 1.7%.

Refinements in the noncentrosymmetric space group $R3c$, allowing movement of cations off special positions did not result in significant shifts or an improvement in the agreement factor in any situation, and we may conclude that there is no evidence from the refinement that the correct space group is not $R\bar{3}c$.

The results for the cation vacancy models are summarized in Table I. All models give the same oxygen positional parameter and an Mn—O distance of 1.965 ± 0.003 Å.

Considering the three limiting defect structures (models 1 to 3), the situation with equal vacancies on both A and B sites (model 1) is slightly favored over that with vacancies on A sites only and transfer of lanthanum to complete the manganese sublattice (model 2), and model 3 which assumes elimination of La_2O_3 to leave vacancies on the A sites only, with perfect manganese and oxygen sublattices.

At this point it was difficult to ascertain the correct situation, although on examination of the ionic radii (*16*) and the Mn—O distance, model 2 seemed unlikely (see Discussion). However, a further improvement is obtained if the metal occupation numbers are varied to generate a situation between the limiting models. If the A-site and B-site occupations are both allowed to vary from model 2 (model 4), an agreement factor of 1.48% is obtained for the stoichiometry $La_{0.95\pm0.02}Mn(La)_{0.96\pm0.04}O_3$. Although there is a slight uncertainty associated with the residual lanthanum on the B site, this strongly indicates a composition between models 1 and 3. Variation of the La^{3+} occupation number from model 3 (model 5) achieves only a small improvement indicating against a complete manganese lattice, although the La^{3+} occupation is increased to 0.94, and assuming a stoichiometry $La_{0.96}Mn_{0.98}O_3$ (model 6) is also no better. Allowing a 2% vacancy concentration on the B sites, and then allowing variation of the La^{3+} occupation (model 7) does however give a significant improvement with a final R factor of 1.45% and composition $La_{0.94\pm0.02}Mn_{0.98}O_3$. A sit-

TABLE II

OBSERVED AND CALCULATED INTENSITIES FOR $La_{0.94\pm0.02}Mn_{0.98}O_{3.00}$

$h\,k\,l$	I_{calc}	$I_{obs}(\times10^{-2})$	$\sigma I_{obs}(\times10^{-2})$
1 1 0	18.19	18.06	0.20
1 0 $\bar{1}$, 1 2 1	1.30	0.87	0.14
2 1 0	16.54	16.48	0.18
2 0 0, 2 2 2	141.11	141.11	0.42
2 2 0	38.26	38.31	0.23
2 0 $\bar{1}$	7.48	7.55	0.15
2 1 $\bar{1}$, 2 3 1	14.98	14.65	0.20
1 1 $\bar{2}$, 3 1 0	0.85	0.83	0.11
3 2 0	5.09	4.78	0.13
2 0 $\bar{2}$, 4 2 2	28.90	29.15	0.25
2 1 $\bar{2}$, 3 1 $\bar{1}$, 4 2 1, 4 3 2, $\bar{1}$ 3 0, 3 3 0, 1 1 4, 4 3 3	38.68	39.68	0.31
3 2 $\bar{1}$, 3 4 1	0.80	2.02	0.16
4 1 0, 2 2 $\bar{2}$, 4 2 0, 2 4 4	90.54	90.27	0.39
4 0 0	5.33	5.49	0.19
4 4 4	4.88	5.54	0.18
3 0 $\bar{2}$, 4 3 0, 3 1 $\bar{2}$, 5 2 2, 3 2 5	26.94	26.95	0.28
2 1 $\bar{3}$, 4 1 $\bar{1}$, 4 5 3, 5 2 1	2.82	1.92	0.16
$\bar{1}$ 4 0, 4 2 $\bar{1}$, 5 3 1, 3 2 $\bar{2}$, 5 4 2	13.23	12.67	0.27
4 4 0	4.01	3.78	0.17

uation with neither the complete Mn lattice of model 3 nor the 4% vacancies of model 1 is thus seen to be most consistent with the neutron diffraction data.

The observed and calculated intensities for the model 7 refinement are given in Table II and the atom positions in Table III (errors quoted to 1σ). It may be noted that the temperature factors follow the same order as in $BaTbO_3$ (*10*) (also a rhombohedral perovskite refined by neutron diffraction), but are somewhat larger which may well reflect the nonstoichiometry in the present compound.

Other Systems

$LaVO_3$, $LaCrO_3$, and $LaFeO_3$

$LaMnO_{3+x}$ is the only system reliably reported where oxidative nonstoichiometry is obtained without doping under readily accessible atmospheric conditions. The refinement reported in this paper, together with that of Pb(La)TiO_3 (*2*) indicates strongly that "excess oxygen" may indeed by incorporated in the perovskite structure by allowing vacancies on the B sites as well as on the A sites. Oxidative nonstoichiometry has not been noticed for other compounds in the much studied systems $LaBO_3$ where B is a first-row transition-metal ion (Ti^{3+} to Cu^{3+}). It is interesting to ascertain whether this reflects a real anomaly (associated with the Jahn–Teller distortion in $LaMnO_3$, for example), or is just an artifact of the preparative conditions normally used. Information on the oxygen stoichiometry of $LaTiO_3$ and $LaVO_3$ is uncertain because of their very ready oxidation, whereas the remaining systems, including $LaCrO_3$ and $LaFeO_3$ resist oxidation under normal conditions.

$LaVO_3$. V_2O_3 was prepared by reduction of V_2O_5 in hydrogen at 900°C for 24 hours and VO_2 by reacting equimolar proportions of V_2O_3 and V_2O_5 in a sealed silica tube at 700°C. The compositions were checked gravimetrically by oxidation to V_2O_5. $LaVO_3$ was prepared by reacting a mixture of dry La_2O_3 and V_2O_3 (mixed in the dry-box) in a vacuum furnace heated internally with a tantalum element. The sample was contained in a tantalum crucible. After two firings at 1200°C

TABLE III

ATOM POSITIONS IN $La_{0.94\pm0.02}Mn_{0.98}O_{3.00}$[a]

Atom		x	y	z	B	Occupation number
2La	2(*a*)	0.25	0.25	0.25	0.92 ± 0.19	1.887 ± 0.038
2Mn	2(*b*)	0.0	0.0	0.0	0.50 ± 0.19	1.96
60	6(*c*)	-0.3024 ± 0.0005	0.8024 ± 0.0005	0.25	1.10 ± 0.11	6.00
		$R(I) = 0.0145$ (19 intensities)				

[a] x, y, z are fractions of the unit cell edges, B is in Å^2.

a product of composition $LaVO_{3.02\pm0.01}$ (checked by oxidation to $LaVO_4$) was obtained. All the lines on a Debye–Scherrer photograph were indexed on an orthorhombic unit cell ($a = 5.551 \pm 0.004$ Å, $b = 5.553 \pm 0.001$ Å, $c = 7.848 \pm 0.006$ Å, $c/\sqrt{2} = 5.549 \pm 0.004$ Å, $V_f = 60.48$ Å^3). This indicates a Jahn–Teller distortion that is small if present at all, as expected from the absence of e_g electrons and also because the covalency in $LaVO_3$ at room temperature seems close to the critical value allowing collective electron behavior (*17*). In $LaMnO_3$ a localized electron scheme is applicable (*18*).

Similar treatment of a mixture of initial composition $LaVO_{3.10}$(La_2O_3:V_2O_3:V_2O_4 = 1:0.8:0.2) gave a final composition $LaVO_{3.07\pm0.01}$ for which a few extra lines were visible in the X-ray photograph. Also, $LaVO_4$ was still present after firing an $LaVO_{3.10}$ mixture from $LaVO_{3.02}$ and $LaVO_4$ in a sealed silica tube at 1200°C. A further firing in the vacuum furnace at 1200°C, however, produced a slightly reduced material of composition $LaVO_{3.05\pm0.01}$ for which all the lines could be indexed ($a = 5.533 \pm 0.005$ Å, $b = 5.544 \pm 0.001$ Å, $c = 7.851 \pm 0.006$ Å, $c/\sqrt{2} = 5.552 \pm 0.004$ Å, $V_f = 60.21$ Å^3).

It would appear, therefore, that incorporation of up to 10% V^{4+} in the $LaVO_3$ cell is permitted. The gravimetric evidence for a change in stoichiometry between $LaVO_{3.02}$ and $LaVO_{3.05}$ is supported by the slight change in lattice parameters and the reduction in V_f. The presence of impurity lines in $LaVO_{3.07}$, however, indicates that the extent of nonstoichiometry in $LaVO_{3+x}$ is significantly less than in $LaMnO_{3+x}$.

$LaCrO_3$. Oxidation of $LaCrO_3$ has not been previously reported, although $LaCrO_4$ has been prepared during decomposition of $La_2(Cr^{VI}O_4)\cdot 8H_2O$ (*19*). Green $LaCrO_3$, prepared by the reaction between La_2O_3 and Cr_2O_3 in air at 1550°C was found to oxidize at 600°C and 130 atm oxygen to a black phase of composition around $LaCrO_{4.4}$ [probably involving oxidation to $LaCrO_4$ and disproportionation to $La_2(CrO_4)_3$], but no evidence was found for nonstoichiometry in the region $LaCrO_{3+x}$. It is possible, however, that under the appropriate pressure conditions the system $La_{0.67-1.0}CrO_{3-4}$ may be interesting.

$LaFeO_3$. Orange $LaFeO_3$, prepared by oxidation of $LaFe(CN)_6$ at 1100°C (*20*) showed no tendency to oxidize at 600°C and 130 atm. oxygen.

$EuTiO_{3+x}$

It has been reported (*5*) that at 1400°C a cubic nonstoichiometric region extends from $Eu^{2+}Ti^{3+}O_{2.5}$ through $Eu^{2+}Ti^{4+}O_{3.0}$ to $Eu^{2+}_{0.48}Eu^{3+}_{0.52}Ti^{4+}O_{3.26}$ (or $Eu_{0.92}Ti_{0.92}O_3$) with only a slight shrinkage of lattice parameter (from 3.90 Å for $EuTiO_{2.5-3.0}$ to 3.88 Å for $EuTiO_{3.26}$ —no errors quoted).

In this work, mixtures of $EuTiO_{3.0}$ and $EuTiO_{3.5}$ corresponding to $EuTiO_{3.1}$ and $EuTiO_{3.2}$ were fired in evacuated silica tubes at 1200°C for 24 hours, but no reaction was observed (cf. $LaVO_{3+x}$). The net composition was unchanged; the starting materials were present with no significant change in lattice parameters; and no third phase was observed. Except for the event that no reaction whatsoever had occurred, it appears that the region

of nonstoichiometry in $EuTiO_{3+x}$ is only extensive above 1200°C. $EuTiO_{3.0}$ (cubic, $a = 3.9044 \pm 0.0002$ Å; composition by weight loss from starting materials and oxidation to $EuTiO_{3.5}$:$EuTiO_{2.990\pm0.005}$) was prepared by hydrogen reduction at 1300°C of dried Eu_2O_3 and TiO_2 (complete reduction did *not* occur at 1200°C), and $EuTiO_{3.5}$ from Eu_2O_3 and TiO_2 in oxygen at 1400°C (cubic, $a = 10.206 \pm 0.001$ Å).

La-Doped $BaTiO_3$ and $SrTiO_3$

The literature concerning the effect of dopant ions on the physical properties of $SrTiO_3$, and especially $BaTiO_3$, is extensive, but little of the work has been concerned with establishing phase diagrams or structural data, although we have noted the study of La^{3+}-doped $PbTiO_3$ (*2*, *13*). Eror and Smyth, however, have reported (*4*) that in $BaTiO_3$ up to 20% barium may be substituted by lanthanum to retain a single phase fully oxidized material (no second phases were observed either optically or by X-ray diffraction). This could be more or less fully reduced (to $Ba_{0.8}La_{0.2}Ti_{0.8}Ti^{4+}_{0.2}O^{3+}_{3.0}$) in carbon monoxide, and the oxidation–reduction process was reversible to the extent of 80% of the predicted weight change. Both phases were claimed to be cubic, the ferroelectric Curie point (see Introduction) of the oxidized material presumably being below room temperature.

In this work the effect of lanthanum substitution in $BaTiO_3$ and $SrTiO_3$ has been studied.

$Ba_{0.8}La_{0.2}TiO_{3.0-3.1}$. Starting materials were $BaCO_3$, La_2O_3 and TiO_2. La_2O_3 and TiO_2 were dried at 1000°C and $BaCO_3$ was heated at 900°C under CO_2 before weighing out. It was not possible to produce a single phase material by firing under oxygen only. Even after two firings at 1400°C and quenching from 1150°C faint extra lines, in addition to the perovskite lines, were visible on an X-ray photograph. A single, simple cubic perovskite phase (accounting for all observed lines) was, however, obtained by subsequent reduction in hydrogen followed by reoxidation in air at 1000°C. This phase was preserved by rereduction in hydrogen at 1150°C, giving a dark blue product. Weight loss indicated a composition $Ba_{0.8}La_{0.2}TiO_{3.01\pm0.01}$. The lattice parameters of the oxidized and reduced materials were 3.991 ± 0.001 Å and 3.985 ± 0.001 Å. As expected the lattice parameter of $Ba_{0.8}La_{0.2}TiO_{3.10}$ is less than that of undoped $BaTiO_3$ {$a = 4.012$ Å at 200°C [above the Curie temperature (*1*)]}. The reduction in V_f (1.6%) is, however, somewhat less than for $LaMnO_{3.0-3.1}$ (3.1%). Intermediate compositions of higher Ti^{4+} content and lighter color were obtained by reduction at lower temperatures.

$Sr_{0.8}La_{0.2}TiO_{3.0-3.1}$. In this case single phase materials could not be obtained. After firing in oxygen at 1500°C, reduction in hydrogen at 1100°C and reoxidation in air at 800°C, La_2O_3 lines were always visible. The reduced and oxidized forms had identical lattice parameters (3.9084 ± 0.0003 Å and 3.9080 ± 0.0003 Å, respectively). This is very close to that of pure $SrTiO_3$ (3.905 Å) and appears to indicate only slight solubility of La^{3+} in $SrTiO_3$.

We have therefore confirmed that a region of oxidative nonstoichiometry exists in lanthanum-doped $BaTiO_3$, at least up to 20% La substitution, but find that La doped $SrTiO_3$ has, on the contrary, no significant range of nonstoichiometry.

Discussion

Lanthanum Manganite

It is clear that powder neutron diffraction is a powerful tool in investigating nonstoichiometry in inorganic systems. This has already been demonstrated, for example, for fluorite systems (*21*), but in the present work we have used the technique to determine a probable defect structure with 6% vacancies on one metal site and only 2% on the other, and to distinguish this from alternative structures which differ in vacancy concentrations by as little as 2%. The refinement also derived an oxygen positional parameter in the presence of heavier metal ions and isotropic temperature factors for the three atoms [c.f.

$Pb(La)TiO_{3+x}$

(*2*) using X-rays where only an overall temperature factor was obtained and all atom positions were fixed by symmetry].

The refinement clearly indicates that a model involving oxide interstitials is very unlikely. Further evidence against such a situation is the absence of diffuse scattering in the neutron pattern. This is in contrast to nonstoichiometric anion-excess fluorite systems (*21*), for example, where the presence of many interstitial ions causes significant local relaxation of ions from special positions and leads to very pronounced diffuse scattering.

The models discussed all assume random vacancies, and there is no evidence from the experiments performed for electronic ordering between Mn^{3+} and Mn^{4+} or for vacancy ordering on either La or Mn sites. A brief electron diffraction study supported the simple perovskite structure derived from the powder studies.

The La_2O_3 eliminated according to the structure refinement was not observed either in Debye–Scherrer X-ray photographs or in the neutron pattern. Such a small amount may have been below the lower limit of detection in this case, may have been converted in the course of exposure to the atmosphere before neutron diffraction to the poorly crystalline hydroxide, or may have been retained within the perovskite matrix in some manner. Any effect on the structure refinement is not considered to be significant.

It is interesting to compare the calculated B site ionic radius with the observed Mn—O bond length (1.965 ± 0.003 Å). Compared to the average Mn—O bond length in $LaMnO_{3.0}$ (2.017 Å) this represents a decrease in overall radius of the B occupants of 0.052 Å.

The effective ionic radii of La^{3+}, Mn^{3+}, and Mn^{4+} in octahedral coordination by oxygen are 1.045 Å, 0.645 Å, and 0.54 Å, respectively (*16*). Using these values we find the average B cation radii for models 2:

$$(La_{0.92}(La_{0.04}Mn^{3+}_{0.73}Mn^{4+}_{0.23})O_3),$$
$$1\,(La_{0.96}(Mn^{3+}_{0.73}Mn^{4+}_{0.23}\square_{0.04})O_3),$$
$$3\,(La_{0.92}(Mn^{3+}_{0.76}Mn^{4+}_{0.24})O_3),$$
$$\text{and } 7\,(La_{0.94}(Mn^{3+}_{0.745}Mn^{4+}_{0.235}\square_{0.02})O_3)$$

to be 0.639 Å, 0.615–0.623 Å, 0.620 Å, and 0.617–0.621 Å, respectively (the uncertainties for models 1 and 7 arise from allowing the vacancy radius to lie between 0.5 Å and 0.7 Å). These represent reductions from the Mn^{3+} radius of 0.006 Å, 0.022–0.030 Å, 0.025 Å, and 0.024–0.028 Å, respectively, all considerably less than the observed decrease. Even assigning zero radius to the vacancy (a very unlikely situation) a decrease of only 0.038 Å is obtained for the observed structure (model 7). The very small decrease calculated for model 2 is additional evidence against this cation distribution, but the similar values calculated for the three cation defect models which do not involve transfer of lanthanum do not allow a choice between them on the basis of ionic radii.

The effective oxygen radius of about 1.37 Å obtained from the Mn—O distance in $LaMnO_{3.0}$ and the Mn^{3+} radius is consistent with oxygen radii estimated for other orthorhombic perovskites (*10*), indicating that 0.645 Å is indeed an appropriate Mn^{3+} radius in this case. The reason for the larger than calculated decrease in Mn—O distance for the oxidized sample is not clear, unless the Mn^{3+} radius decreases in going from $LaMnO_{3.0}$ with long-range Jahn–Teller ordering to the rhombohedral perovskites with no such long-range order.

The preparation of compositions of higher oxygen content than $LaMnO_{3.12}$ required lower temperatures and sometimes higher pressure of oxygen, and the X-ray evidence indicates the structures to be more complicated. The retention of the basic rhombohedral lattice and the relation of the new lines to a perovskite cell suggest some ordering process, although this aspect was not pursued in the investigation being reported.

For rhombohedral perovskites we find a simple relation, $\tan \omega = \sqrt{12}t$, between the movement t of the oxygen atoms off the special positions and the angle of rotation ω of the octahedra about the $\langle 111 \rangle$ axis. In the present case $t = 0.0524$ giving $\omega = 10°17'$. Using the relation derived by Moreau et al. (*22*) between ω and $\Delta\alpha$, the distortion of the rhombohedral cell angle from 60°, we find α to be 60°43′, in very good agreement with the observed value of 60°40′.

Using these relations we estimate the Mn—O bond length in $LaMnO_{3.20}$ to be 1.95 Å, a relatively small decrease from $LaMnO_{3.12}$ as might be anticipated. The distortion from cubic symmetry is smaller than for $LaMnO_{3.12}$ (30′ cf. 40′) because of the further reduction in Mn—O distance.

Oxidative Nonstoichiometry in Other Systems and Comparison with $LaMnO_{3+x}$

On the basis of powder X-ray diffraction evidence and, in particular, from the variations of lattice parameter with composition, it appears that the $LaVO_{3.0}$ phase can extend only to $LaVO_{3.05\pm0.01}$ (containing 10% V^{4+}), although the means of accomplishing this was not investigated. Nonstoichiometry was not observed for $LaCrO_3$ or $LaFeO_3$.

$LaMnO_{3+x}$, therefore, is apparently the only system in the lanthanum-transition-metal perovskites which exhibits a wide range of oxidative nonstoichiometry. At least 20% La^{3+} can be substituted for Ba^{2+} in $BaTiO_3$ to produce a single phase region over the range

$$Ba^{2+}_{0.8}La^{3+}_{0.2}Ti^{4+}_{1.0}O_{3.10}$$

$$\text{to } Ba^{2+}_{0.8}La^{3+}_{0.2}Ti^{4+}_{0.8}Ti^{3+}_{0.2}O_{3.0}.$$

The maximum extent of lanthanum substitution was not established, although the preparation indicated that the nonstoichiometric phase was possibly not stable at high temperature. In contrast, the extent of substitution of La^{3+} in $SrTiO_3$ was very small. The nonstoichiometric region reported for $EuTiO_3$ was not observed by reaction at or 1200°C below.

It is unlikely that the oxidative nonstoichiometry of $Ba_{0.8}La_{0.2}TiO_{3.10}$ can be explained by simple elimination of La_2O_3 or BaO to give $(Ba_{0.8}La_{0.137}\square_{0.067})Ti^{4+}O_3$ or $(Ba_{0.7}La_{0.2}\square_{0.1})Ti^{4+}O_3$. Although no special precautions were taken to exclude moisture from the samples, the experience with $Sr_{0.8}La_{0.2}TiO_{3.1}$ indicates that La_2O_3 can be observed under these circumstances, and moreover, the reversible oxidation–reduction behavior observed by Eror and Smyth (*4*), and in this work at temperatures between 600° and 1100°C, would be improbable in such a situation where production of anion vacancies would then be involved. Significant reduction of $SrTiO_3$ and $BaTiO_3$ even in hydrogen is not straightforward.

It is generally observed that upon oxidation, perovskites ABO_3 convert to a more highly oxidized phase of stoichiometry $ABO_{3.5}$ or ABO_4 (e.g., $LaTi^{3+}O_3 \rightarrow La_2Ti^{4+}_2O_7$, $LaV^{3+}O_3 \rightarrow LaV^{5+}O_4$, and $Eu^{2+}Ti^{4+}O_3 \rightarrow Eu^{3+}_2Ti^{4+}_2O_7$), although the finer details of such phase changes at the perovskite end have not always been investigated thoroughly. We now have evidence that in at least three situations—$LaMnO_{3+x}$, La-doped $PbTiO_3$, and La-doped $BaTiO_3$—but apparently not in several others, the extra oxygen, available by oxidation or cation substitution, may be accommodated over a considerable range of oxidative nonstoichiometry by the introduction of defects on both metal lattices together with, in some cases, partial elimination of the A site metal oxide which has the effect of reducing the B site vacancy concentration at the expense of A site vacancies. In the absence of thermodynamic information, an oxidation which produces a defect perovskite and a metal oxide, e.g.,

$$LaMn^{3+}O_3 \rightarrow La_{2/3}\,Mn^{4+}O_3 + \tfrac{1}{6}\,La_2O_3 \quad (4)$$

could be considered as likely as the production of $ABO_{3.5}$ or ABO_4 phases, but such a situation is not generally observed (although the occurrence of phases of the type $La_{1-x}M^{3+}_{1-3x}M^{4+}_{3x}O_3$ is not apparently rare). The production of B site vacancies has, however, been thought to be both extremely unlikely, and, until very recently, unobserved.

We must note that very little thermodynamic information exists for the compounds studied here, and we may not necessarily be observing a state of thermodynamic equilibrium—not an unusual uncertainty in solid state chemistry. Also, in the studies of phases of the type $A_{1-x}BO_3$ mentioned above and of the materials with B site vacancies, the phase limits, vacancy compositions, and unit cell dimensions are by no means always definitively established. More detailed investigations looking for long-range order or defect clustering, for example, have hardly been carried out at

TABLE IV

SOME IONIC RADII RELEVANT TO OXIDATIVE NONSTOICHIOMETRY IN PEROVSKITES (Å)[a,b]

Lower oxidation state ion		Higher oxidation state ion		% Decrease in radius
$^{XII}Ba^{2+}$	1.60	$^{XII}La^{3+}$	1.32	17.5
$^{VI}Mn^{3+}$	0.645	$^{VI}Mn^{4+}$	0.540	16.3
$^{VIII}Eu^{2+}$	1.25[c]	$^{VIII}Eu^{3+}$	1.07	14.4
$^{XII}Pb^{2+}$	1.49	$^{XII}La^{3+}$	1.32	11.4
$^{VI}Cr^{3+}$	0.615	$^{VI}Cr^{4+}$	0.55	10.6
$^{VI}Ti^{3+}$	0.67	$^{VI}Ti^{4+}$	0.605	9.7
$^{VI}V^{3+}$	0.640	$^{VI}V^{4+}$	0.59	7.8
$^{VI}Cr^{2+}$	0.82	$^{VI}Cr^{3+}$	0.615	25.0
$^{VI}Ti^{4+}$	0.605	$^{VI}Nb^{5+}$	0.64	−5.8

[a] Values taken from (*16*).

[b] The coordination numbers are indicated by Roman superscripts.

[c] The appropriate coordination number for Eu is XII but radii are tabulated only up to VIII coordination.

all. However, one factor which appears to be common to all three systems to which B site vacancies have been assigned is that the higher oxidation state ion responsible for the nonstoichiometry is significantly smaller than the host cation. Some relative sizes are indicated in Table IV. A relatively rapid increase in lattice energy upon oxidation or doping may be a stabilizing factor for B site vacancies. In this case we may expect that $EuTiO_{3+x}$ will show such nonstoichiometry under suitable conditions, but that doping $BaTiO_3$ with Nb^{5+} (to substitute for Ti^{4+} on the B sites) will be ineffective in this regard.

Certainly Ba^{2+}/La^{3+} and Mn^{3+}/Mn^{4+} show very large radius decreases, and that for Pb^{2+}/La^{3+} is larger than for the other transition-metal pairs. Thus the reason for the unusual behavior of $LaMnO_{3+x}$ compared to the other compounds in the $LaBO_3$ transition metal series may well be associated with the loss from Mn^{3+} on oxidation of the single e_g σ-antibonding electron, responsible for the Jahn–Teller distortion, which results in such a large decrease in ionic radius. We see from Table IV that a study of the oxidation of fluoride perovskites containing Cr^{2+}, also a d^4 Jahn–Teller ion, (e.g., $KCrF_{3+x}$) may be interesting—perhaps compositions with B site vacancies can be prepared in addition to the "bronzes" $K_{1-x}CrF_3$ (*23*).

Of course, the formation of alternative phases may be favored in any particular system, and the reluctance of $LaMnO_{3+x}$ to form more highly oxidized nonperovskite phases (or possibly $La_{1-x}MnO_3$ phases which may be less stable in comparison to $La_{1-x}VO_3$ and $La_{1-x}TiO_3$) may be a factor in permitting the formation of such a wide nonstoichiometric region. It does not necessarily follow that other phases showing oxidative nonstoichiometry need be structurally analogous to $LaMnO_{3.12}$, and indeed in this system, more complex behavior is observed in samples of higher Mn^{4+} content. The X-ray powder technique, however, is much less useful than neutron or electron diffraction for detailed investigation of such nonstoichiometric systems, and we may note that a preliminary survey of $Ba_{0.8}La_{0.2}TiO_{3.1}$ by electron diffraction (to be reported later) seems to indicate the presence of superlattice ordering, although the powder photograph shows only lines characteristic of a simple cubic cell.

Acknowledgments

We would like to thank Professor J. S. Anderson for use of the tantalum furnace, and Dr. B. E. F. Fender, the Science Research Council, A.E.R.E., Harwell and the University Support Group there for provision of neutron facilities. We are deeply indebted to Dr. A. J. Jacobson for performing the refinements on the models allowing for oxide elimination.

References

1. J. B. GOODENOUGH AND J. M. LONGO, *in* "Landolt-Börnstein, Numerical Data and Functional Data in Science and Technology." New Series. (K. H. Hellwege, Ed.), Group III, Vol. 4a, p. 131. Springer-Verlag, New York (1970).
2. D. HENNINGS AND G. ROSENSTEIN, *Mat. Res. Bull.* 7, 1505 (1972).
3. A. WOLD AND R. J. ARNOTT, *J. Phys. Chem. Solids* 9, 176 (1959).
4. N. G. EROR AND D. M. SMYTH, *in* "The Chemistry of Extended Defects in Non-metallic Solids" (L. Eyring and M. O'Keeffe, Eds.), p. 62, North-Holland, Amsterdam (1970).

5. G. J. McCarthy, W. B. White, and R. Roy, *J. Inorg. Nucl. Chem.* **31**, 329 (1969).
6. B. T. M. Willis, *in* "Thermodynamic and Transport Properties of Uranium Dioxide and Related Phases," Chap. II. International Atomic Energy Agency, Vienna (1965).
7. E. G. Steward and H. P. Rooksby, *Acta Cryst.* **4**, 503 (1951).
8. J. B. A. A. Elemans, B. Van Laar, K. R. Van der Veen, and B. O. Loopstra, *J. Solid State Chem.* **3**, 238 (1971).
9. B. C. Frazer, H. R. Danner, and R. Pepinsky, *Phys. Rev.* **100**, 745 (1955).
10. A. J. Jacobson, B. C. Tofield, and B. E. F. Fender, *Acta Cryst.* **B28**, 956 (1972).
11. M. Kestigian, J. G. Dickinson, and R. Ward, *J. Amer. Chem. Soc.* **79**, 5598 (1957).
12. P. Dougier and A. Casalot, *J. Solid State Chem.* **2**, 396 (1970).
13. D. Hennings and K. H. Härdtl, *Phys. Status Solidi* (a)**3**, 465 (1970).
14. The Neutron Diffraction Commission, *Acta Cryst.* **A25**, 391 (1969).
15. A. J. Jacobson, B. C. Tofield, and B. E. F. Fender, *J. Phys. C.* (*Solid State Physics*) **6**, 1615 (1973).
16. R. D. Shannon and C. T. Prewitt, *Acta Cryst.* **B25**, 925 (1969); **B26**, 1046 (1970).
17. D. B. Rogers, A. Ferretti, D. H. Ridgley, R. J. Arnott, and J. B. Goodenough, *J. Appl. Phys.* **37**, 1431 (1966).
18. J. B. Goodenough, *J. Appl. Phys.* **37**, 1415 (1966).
19. H. Schwarz, *Z. anorg. allgem. Chem.* **322**, 1 (1963).
20. P. K. Gallagher, *Mat. Res. Bull.* **3**, 225 (1968).
21. A. K. Cheetham, B. E. F. Fender, and M. J. Cooper, *J. Phys. C.* (*Solid State Physics*) **4**, 3107 (1971).
22. J. M. Moreau, C. Michel, R. Gerson, and W. J. James, *Acta Cryst.* **B26**, 1425 (1970).
23. D. Dumora, J. Ravez, and P. Hagenmuller, *J. Solid State Chem.* **5**, 35 (1972).